Cracks and Topological Defects in Lyotropic Nematic Gels

M. F. Islam,* M. Nobili,† Fangfu Ye, T. C. Lubensky, and A. G. Yodh

Department of Physics and Astronomy, University of Pennsylvania, 209 S. 33rd Street, Philadelphia, Pennsylvania 19104-6396, USA

(Received 19 January 2005; published 26 September 2005)

We report on the effects of the coupling of nematic order and elasticity in anisotropic lyotropic gels consisting of large nematic domains of surfactant coated single wall carbon nanotubes embedded in a cross-linked *N*-isopropyl acrylamide polymer matrix. We observe the following striking features: (i) undulations and then cusping of the gel sidewalls, (ii) a nematic director field that evolves as the gel sidewalls deform, (iii) networks of surface cracks that are orthogonal to the nematic director field, and (iv) fissures at the sidewall cusps and associated topological defects that would not form in liquid nematics.

DOI: 10.1103/PhysRevLett.95.148301 PACS numbers: 82.70.Gg, 64.70.Md, 81.05.Qk, 81.07.Bc

Topological defects and cracks are common in many condensed matter systems. Quenching and frustration induce various types of defects in liquid crystals and crystalline solids [1,2], and cracks arise from external and internal stresses in crystalline [3,4] and amorphous solids [5–8]. We explore the formation of cracks and defects in lyotropic nematic gels, materials that couple orientational ordering of embedded rods to an amorphous cross-linked polymer matrix. Thermotropic analogs of these materials have unique elastic properties [9] that make them candidates for use as actuators and artificial muscles [10–13]. Typically, these thermotropic materials are synthesized in a two-step process [9] of polymerization and cross-linking of liquid crystalline organic monomers followed by a second cross-linking under external stress. They do not exhibit topological defects because the strong coupling between the nematic director [14] and network elasticity makes their formation energetically unfavorable [9]. In addition, crack formation in the absence of external stress has not been observed in the thermotropic gels.

Herein, we investigate crack formation and defects in freestanding lyotropic nematic gels. These gels are amorphous solids of cross-linked *N*-isopropyl acrylamide (NIPA) polymer matrix with large embedded liquid crystalline domains of surfactant coated single wall carbon nanotubes (SWNTs). The alignment of SWNTs in these gels is larger near the gel surfaces than in the bulk [15], the sidewalls of these nematic nanotube gels exhibit undulations and cusps, and the nematic director exhibits associated anomalous modulations [16]. Surprisingly, we observe networks of surface cracks orthogonal to the nematic director field and fissures with associated $+1$ topological defects in these gels, even though there are no external stresses. We propose that an internal stress, arising from the coupling between the nematic order of SWNTs within the gel and the polymer network elasticity, causes cracks and defects to form. To the best of our knowledge, this is the first observation of crack formation in a solid induced by an internal tensorial field, in this case by nematic order.

Lyotropic nematic gels were prepared by first dispersing SWNTs in water using an anionic surfactant sodium dodecyl benzene sulfonate (NaDDBS, $C_{12}H_{25}C_6H_4SO_3Na$) [17]. These SWNTs are long and thin with an average length $L = 516 \pm 286$ nm and average diameter $d \sim 1.35 \pm 0.15$ nm [17]. The SWNT suspension and NIPA polymer ingredients (NIPA monomer, cross-linker, initiator, and stabilizer) were mixed and vortexed, loaded into rectangular capillary tubes, and polymerized at 295 K for $\sim$3 hours. Details of the gel preparation and the nanotube distribution in the gel can be found elsewhere [15]. The two ends of the capillary tubes were sealed with optical glue, taking care to avoid trapping air bubbles. Then samples were placed on a heated optical microscope stage at 338 K for observation. At this temperature, the NIPA network became hydrophobic, and the gels experienced a volume compression of $\sim 8\times$, expelling water in the process. The dimensions of the shrunken gels were $\sim$2 cm $\times$ 2 mm $\times$ 0.1 mm. The nanotube concentration in the shrunken SWNT-NIPA gels (c_{SWNT}) was 8.25 mg/ml, greater than the critical concentration for the isotropic-nematic transition of our SWNTs in the gel of $\sim$3.3 mg/ml [15]. Sealing the capillary tubes prevented water evaporation and drying.

We studied the evolution of these *shrunken* gel physical properties and determined the nematic director orientations using bright-field, conoscopic, and polarizing microscopy. We made our observations with a Leica DMIRB inverted optical microscope and recorded images with a CCD camera (640 $\times$ 480 pixels) and an 8-bit video frame grabber.

Conoscopic microscopy [18] was used to determine whether the lyotropic rods have planar (parallel to XY plane; axes defined in Fig. 1) or homeotropic (parallel to Z axis) alignment. In these measurements, the gels were inserted between crossed linear polarizers with their directors at 45° relative to the polarizer pass axes, and illuminated with light ($\lambda = 546$ nm). An interference pattern, produced as a result of the phase difference between the ordinary and extraordinary waves passing through the sample, will contain two sets of dark hyperbolas, characteristic of planar alignment, or concentric circular fringes

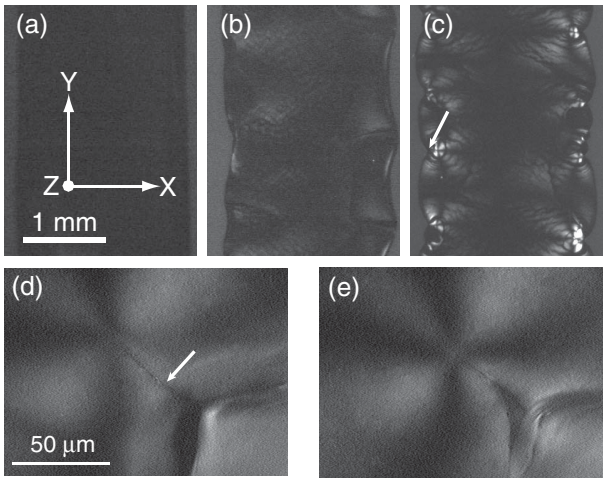

FIG. 1. (a)–(c) A summary of the evolution of the physical properties of the nematic gels with time before and after shrinking. The gel sidewalls remained flat for a few minutes to several hours after the gels have shrunk (a). Undulation of the gel sidewalls developed within a few hours to 1 day (b). We also observed surface cracks [dark lines in (b)]. The undulations eventually gave rise to sidewall cusps, indicated by an arrow in (c). (d)–(e) Fissures developed at the sidewall cusp and propagated along the X axis into the sample and along the Z axis the entire thickness of the gel, indicated by an arrow in (d). Radial $+1$ defect is clearly visible 36 μm (d) and 51 μm (e) along the Z axis into the sample.

with an extinction cross, characteristic of homeotropic alignment [18]. The projection of the nematic director into the XY plane was very uniform, permitting conoscopic measurements throughout the gel except directly on the defects. These measurements showed two sets of dark hyperbolas. Thus, the nematic director had planar or nearly planar orientation.

Semiquantitative information about SWNT alignment in the gels were obtained from images of sample birefringence. Isotropic regions and those with nematic director aligned along one of the crossed linear polarizer axes appear dark. Regions with nematic director aligned in the plane of the polarizers and oriented at $\pm 45°$ with respect to the polarizer pass axes appeared brightest. To remove this twofold degeneracy, we illuminated these bright regions with light ($\lambda = 546$ nm), and then inserted a $\lambda/4$-wave plate between the polarizer and the sample. The slow axis of the $\lambda/4$-wave plate was oriented at $+45°$ with respect to the polarizer pass axis. We then measured the transmitted intensities parallel (I_+) and perpendicular (I_-) to the slow axis of the $\lambda/4$-wave plate, where:

$$I_\pm = \frac{I_\parallel}{4} + \frac{I_\perp}{4} \pm \sqrt{\frac{I_\parallel I_\perp}{4}} \sin\phi. \quad (1)$$

In Eq. (1), $I_\parallel$ and $I_\perp$ depend on the anisotropic absorption cross section of SWNTs [19]; they are the transmitted intensities of light polarized parallel and perpendicular to the director, respectively. ϕ is the optical dephasing angle due to the anisotropic index of refraction of SWNTs [20]. The maximum birefringence (Δn) of our four-day-old gel samples with thickness $d = 100$ μm was less than 5×10^{-4}, corresponding to an optical dephasing of less than $\pi/5$ ($\phi = 2\pi\Delta n d/\lambda$). In this regime of a weak dephasing ($\phi < \pi$), I_+ is larger than I_-. Thus, we removed the twofold degeneracy and quantitatively mapped the director field.

Observations of the time dependence of the physical properties of the gels are illustrated in Figs. 1(a)–1(c). Before shrinking, the gels were isotropic and the gel walls were flat [Fig. 1(a)]. After shrinking, the gels remained isotropic and the gel walls remained flat for a few minutes to several hours. Thereafter, nanotubes in the gels started to order, and the gels started to become birefringent. Birefringence was stronger near the edges of the gels. Eventually, the gel sidewalls started to undulate [Fig. 1(b)]; the time scale for development of undulation varied from a few hours to 1 day. Within a few hours after shrinking, we observed the development of cracks with a depth (along Z axis) of ~ 10 μm on the top and bottom gel surfaces [dark lines in Figs. 1(b) and 1(c)]. These surface cracks continued to evolve over the next 4 days. During the next 1 to 3 days, the undulations evolved to cusplike modulations [Fig. 1(c)]; the undulations and cusps of the sidewalls were symmetric along the Z axis. Soon after, fissures developed at the location of each cusp and propagated along the X axis into the gels. The fissures were $40-50$ μm long with a depth along the Z axis of the entire thickness of the gels. In Figs. 1(d) and 1(e) we show pictures of a fissure between crossed polarizers at 36 μm and 51 μm along the Z axis into the sample. At the tip of each fissure, we observed an associated point defect [clearly visible in Fig. 1(d) and 1(e)]. The fissures were oblique with respect to the Z axis, as can be seen in Figs. 1(d) and 1(e). The top and the bottom surfaces also showed smooth in-phase undulations which resulted in a sinusoidal bending of the whole sample. We did not observe additional evolution of the gels after four days. In contrast, the gel walls of shunken NIPA gels with SWNT concentrations below c_{crit} (including zero) did not undulate or form cusps, fissures, and surface cracks [15]. Thus, the deformations we have observed are not a result of inhomogeneous shrinking of the NIPA gel, as has been observed in various contexts in the past [21].

To determine the type and strength of the point defects, we again inserted the gels between crossed polarizers. The four bright lobes associated with each defect suggest that the strength of the defects are $+1$ or -1 [1]. To determine the sign of the defects (i.e., $+1$ or -1), the position of the sample was kept fixed and the crossed polarizers were rotated counterclockwise in steps of 15°. The extinction branches for every defect rotated in the same sense as the polarizers suggesting the defects were $+1$. In Fig. 2 we show the counterclockwise rotation of the defect lobes with a counterclockwise rotation of crossed polarizers. Furthermore, by mapping the director field around the

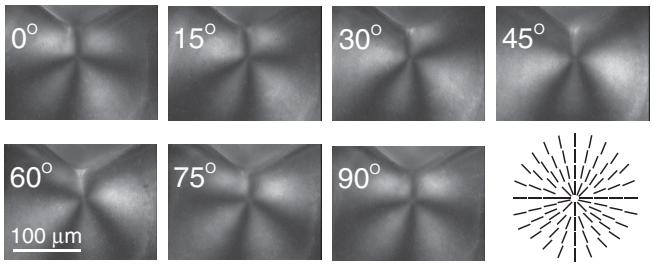

FIG. 2. The four bright lobes of the defects rotated counterclockwise with a counterclockwise rotation of the crossed polarizers suggesting the defects are +1. The SWNT orientation and the director field around the +1 defects were radial (shown schematically on right).

defects using polarization microscopy and a $\lambda/4$-wave plate, we determined that the director field around all point defects had radial orientation as sketched in Fig. 2.

To elucidate how the director field in these lyotropic nematic nanotube gels evolves to create radial +1 defects, we measured the director field as a function of time while the gel sidewalls evolved from undulated to cusplike. At all stages of the gel evolution, the nematic director in the middle of the gel lay along the Y axis; the director was also parallel to gel surfaces. When the gel sidewalls developed undulations, the director field near the gel walls followed the undulation. This surface induced director modulation relaxed within $\sim 50-100$ μm along the X axis into the sample. Surprisingly, further into the gel we observed a second modulation of the director field 180° out of phase with the first modulation. This second modulation then relaxed within ~ 100 μm to the uniform nematic director at the middle of the gel. In Fig. 3 we show a birefringent image of a shrunken gel with undulated free surface and sketch the corresponding director field. Notice that, except for the gray shaded region in Fig. 3(b), the two director modulations at the concave part combine to give a director field equivalent to a field of a +1 defect. After cusping and fissure formation, the director in this region assumed an orientation parallel to the free surfaces of the fissure [Fig. 3(c)]. The final director field was that of a radial +1 defect [Fig. 3(d)]. The fissures create surfaces that are essentially perpendicular to the original undeformed surfaces of the gels. The simplest director configuration that satisfies the boundary conditions of being parallel to the fissure surfaces along them (i.e., along the X axis) and decaying to the perpendicular alignment in the sample center (i.e., along the Y axis) is a $+1/2$ defect centered at the fissure termination. This configuration would be energetically favored in fluid nematics with no shear elasticity. Interestingly, our observations show that +1 rather than $+1/2$ defects develop from the director modulation before cusping.

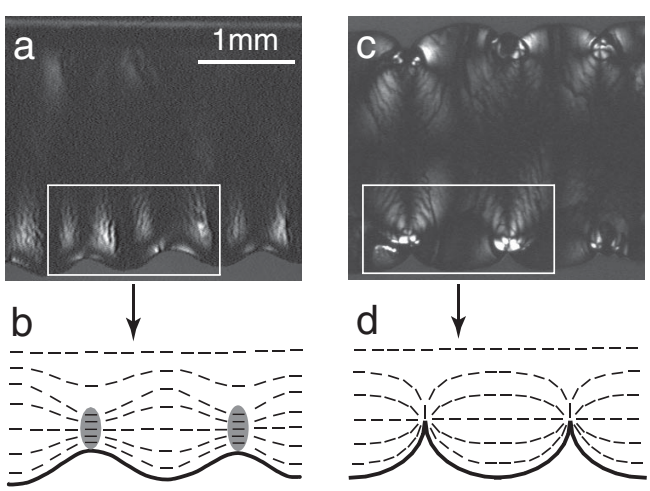

FIG. 3. Birefringence images and sketches of the director field in gels during undulations but before cusping [(a) and (b)] and after cusping [(c) and (d)].

The lyotropic nematic gels exhibit another fascinating property. If we overlay the director field shown in Fig. 3(d) on the image of the network of surface cracks in Fig. 4(a), we find the surface cracks are orthogonal to the nematic director field [Fig. 4(b)]. For example, near the middle of the gel and near the sidewalls away from the defects, the director field lies along the Y axis and the surface cracks are along the X axis [Fig. 4(a)]. We also find the crack pathways deviate as they approach the radial +1 defect and form circular patterns [Fig. 4]. Similar deviations of crack propagation by defects have been observed in brittle solids [4]. Interestingly, the surface cracks provide us with an-

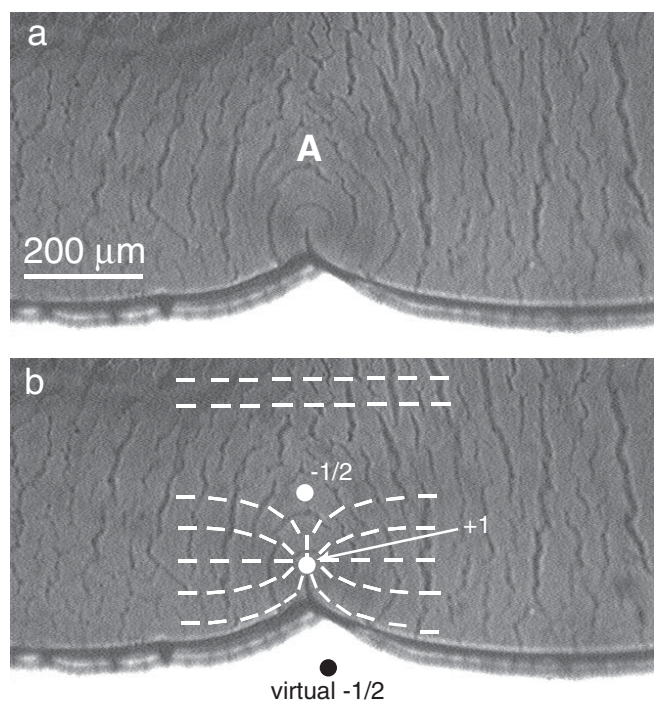

FIG. 4. (a) Surface cracks develop in the nematic gels after 4 hours to 1 day. (b) Overlaying the director field on the crack pathways, we find that the surface cracks are orthogonal to the director field. The crack pathways also suggest the presence of a $-1/2$ defect at region **A**.

other route to map the director field in the gel. In particular, the surface crack field suggests the presence of $-1/2$-like defects in region **A** of Fig. 4(a). Mapping of the director field also indicated the presence of $-1/2$ defects in region **A**. We did not see any depolarized diffusion of light associated with a $-1/2$ defect core between crossed polarizers, but the same region **A** always appeared dark between crossed polarizers. It is likely that the core of these $-1/2$ defects is smeared out to a few microns because of the large length of SWNTs (few hundred nanometers) compared to that of conventional thermotropic liquid crystals (few nanometers). In addition, the optical signature of the depolarized light diffusion from the core could be very weak and its presence not easily detectable.

We propose a simple explanation for our observations. After the gel completely shrinks and the concentration of SWNTs in the gel becomes larger than c_{crit}, the SWNTs in the gel start to align. The gel walls provide an aligning field for the SWNTs. Consequently, the nematic order parameter becomes larger near the gel surfaces than in the bulk. At this stage, the nematic order of SWNTs competes with the polymer network elasticity. The coupling between the nematic director and the network elasticity gives rise to an internal tensile stress parallel to the director field. This internal tensile stress causes the gel to stretch more near the surface than in the bulk, leading to an undulation of the free surface (buckling instability), eventually forming cusps and fissures. The same stress also induces cracks on the gel surfaces with the crack pathways being orthogonal to the nematic director [22]. The penetration depth of both the fissures and the cracks are possibly related to the gradient of the nematic order parameter.

Though complete theoretical modeling of the final defect and crack structure is difficult, we have been able to demonstrate [23], following procedures similar in spirit to those of Ref. [24], that a nematic elastomer with a free surface will undergo a bucklinglike transition when compressed for appropriate values of shear rigidity and small values of the semisoftness parameter [25], which produces a nonvanishing value for the modulus for shears in the plane of the director. The surface shape and director configuration of the unstable buckling mode approximate that shown in Fig. 3(b). It is reasonable that the configuration of Fig. 3(d) will evolve from that of Fig. 3(b) when buckling is fully developed.

If we interpret the defect that forms at the crack tip as having a charge of $+1$, it must be accompanied by a charge -1 or two charge $-1/2$ defects. A $-1/2$ defect can be identified inside the gel [Fig. 4(b)]. The director configuration at the surface can be interpreted as arising from a virtual $-1/2$ defect outside the sample to give two $-1/2$ defects. Alternatively, the defect at the crack tip can be viewed as a boojum [26] on a surface cusp with an effective $-1/2$ winding number to compensate the bulk $+1/2$ defect.

In summary, we have found that cracks and topological defects form in nematic nanotube gels due to the coupling between the nematic order and the elasticity of the polymer network. Our findings can have important implications in the use of lyotropic nematic elastomers and gels as actuators or artificial muscles.

We thank R. D. Kamien and M. Warner for useful discussions. This work has been partially supported by the NSF through the MRSEC Grants No. DMR 00-79909 and No. DMR-0203378 and by NASA, Grant No. NAG8-2172.

*Present Address: Department of Chemical Engineering and Department of Materials Science and Engineering, Carnegie Mellon University, Pittsburgh, PA 15213-3890.
†Permanent Address: Groupe de Dynamique des Phases Condensées, CNRS-Université Montpellier II, Place E. Bataillon, 34090 Montpellier, France.

[1] P. M. Chaikin and T. C. Lubensky, *Principles of Condensed Matter Physics* (Cambridge University Press, Cambridge, England, 1997), 2nd ed.
[2] Z. Tan *et al.*, Macromolecules **32**, 7172 (1999).
[3] B. Lawn, *Fracture of Brittle Solids* (Cambridge University Press, Cambridge, England, 1993).
[4] D. Shilo *et al.*, Phys. Rev. Lett. **89**, 235504 (2002).
[5] K. Shorlin *et al.*, Phys. Rev. E **61**, 6950 (2000).
[6] Z. Neda *et al.*, Phys. Rev. Lett. **88**, 095502 (2002).
[7] E. R. Dufresne *et al.*, Phys. Rev. Lett. **91**, 224501 (2003).
[8] L. Pauchard *et al.*, Phys. Rev. E **67**, 027103 (2003).
[9] M. Warner and E. M. Terentjev, *Liquid Crystal Elastomer* (Oxford University Press, New York, 2003).
[10] C. C. Chang *et al.*, Phys. Rev. E **56**, 595 (1997).
[11] Y. Mao and M. Warner, Phys. Rev. Lett. **86**, 5309 (2001).
[12] H. Finkelmann *et al.*, Phys. Rev. Lett. **87**, 015501 (2001).
[13] J. V. Selinger *et al.*, Phys. Rev. Lett. **89**, 225701 (2002).
[14] Here the nematic director represents the average orientation of the larger polarization axis of the liquid crystalline organic monomers.
[15] M. F. Islam *et al.*, Phys. Rev. Lett. **92**, 088303 (2004).
[16] In these nematic nanotube gels, the nematic director is the average orientation of the long axis of SWNTs.
[17] M. F. Islam *et al.*, Nano Lett. **3**, 269 (2003).
[18] M. Born and E. Wolf, *Principles of Optics* (Cambridge University Press, Cambridge, England, 1980), 6th ed.
[19] M. F. Islam *et al.*, Phys. Rev. Lett. **93**, 037404 (2004).
[20] M. F. Lin, Phys. Rev. B **62**, 13153 (2000).
[21] E. S. Matsuo and T. Tanaka, Nature (London) **358**, 482 (1992); S. Sasaki and H. Maeda, J. Chem. Phys. **111**, 360 (1999); A. Suzuki *et al.*, J. Colloid Interface Sci. **211**, 204 (1999).
[22] R. Duggal, F. Hussain, and M. Pasqualli, Adv. Mat. (in press).
[23] Fangfu Ye and T. C. Lubensky (to be published).
[24] E. M. Terentjev *et al.*, Phys. Rev. E **60**, 1872 (1999).
[25] H. Finkelmann *et al.*, J. Phys. II **7**, 1059 (1997).
[26] N. D. Mermin, in *Quantum Fluids and Solids*, edited by S. B. Trickey, E. Adams, and J. Duffy (Plenum, New York, 1977).